Journal of Engineering and Computer Sciences
Vol. 17, No. 02, pp. 1 - 20 (July-Dec 2025)

Application of Response Surface Methodology for Predicting the Compressive Strength of Mortars Containing Natural Pozzolan

Hany A. Dahish
Department of Civil Engineering, College of Engineering, Qassim University, Buraidah 52571, Saudi Arabia.
E: ha.dahish@qu.edu.sa

Ahmed F. Elragi *
Department of Civil Engineering, College of Engineering, Qassim University, Buraidah 52571, Saudi Arabia.
E: a.elragi@qu.edu.sa

[Received: 25 December 2025, Revised: 09 January 2026, Accepted: 18 January 2026, Published Feb 2026]

Abstract: In this paper, the effect of the inclusion of natural pozzolan (NP) on the compressive strength of cement mortar is investigated. Prediction models of compressive strength of cement mortars having NP were developed utilizing response surface methodology (RSM). In addition, multi-objective optimization has been performed by maximizing the compressive strength with natural pozzolan replacing cement (NPC) in ranges between 0 and 40% by weight of cement and natural pozzolan replacing sand (NPS) in ranges between 0 and 40% by volume of sand. To reduce the negative impact of NP on the compressive strength, silica fume (SF) was used as a partial replacement for cement by weight with ratios of 5% and 10%. The experimental data comprises the 28-day compressive strength of twenty-three mortar mixes. The specimens have cubic shapes with dimensions of 50×50×50 mm. The experimental results were used as the database for developing prediction models to evaluate the impact of doses of NP and SF on NP mortar's compressive strength. Developed models were assessed and validated to check significance and suitability of these combinations in mortar. The involvement of every parameter was analyzed using ANOVA and other statistical measures. Optimal relationships were identified between compressive strength and NPC and/or NPS ratios. The ideal replacement levels of NP for enhancing the NP mortars compressive strength were determined by numerical optimization. Constructed models' outcomes aligned well with experimental data. The predicting NP mortars compressive strength quadratic model outperforms the linear model. Models established in this study can predict compressive strength of cement mortars using NP and SF, the results of which will be highly useful for engineering community.

Keywords*:* Compressive strength; natural pozzolan; silica fume; prediction; response surface methodology; optimization

1. INTRODUCTION

Concrete can be considered as complex building material for its exceptional resistance to compressive loads and its longevity. Portland cement is extensively employed in the construction industry; however, it significantly contributes to energy consumption and environmental degradation due to the detrimental carbon dioxide emissions produced during its manufacturing process. Green concrete is essential to mitigate greenhouse gas releases. Alongside emitting carbon dioxide, cement production generates hazardous dust that adversely impacts the environment and contributes to respiratory illnesses in individuals. The cement industry is also held responsible for the loss of irreplaceable resources such as clay, limestone, and fossil fuels [1]. The cement sector, while important for infrastructural and economic growth, faces substantial environmental difficulties due to its varied emission outputs [2]. It is crucial to prioritize the optimal utilization of resources to substitute conventional ingredients in cement production having natural resources, wastes, or by-products. In response to increasing necessity toward mitigating adverse effects of carbon dioxide emissions, numerous substitute materials were developed as partial replacement for cement. Incorporation of additional cementitious materials

(SCM) in concrete has decreased total expenses, energy consumption, and CO_2 emissions [3–6]. Silica fume is one of the most efficient pozzolanic substances. Substituting up to 7.5% of cement content with silica fume enhanced the compressive strength of concrete [7]. The inclusion of 30% fly ash and 7.5% silica fume substituting cement demonstrated concrete greatest splitting tensile and flexural strengths [8]. Substituting up to 20% of cement by activated low calcium fly ash does not result in a noticeable reduction in mechanical characteristics compared to the control sample [9].

The inclusion of recycled fine aggregate augmented drying shrinkage and diminished compressive strength [9]. Substituting natural river sand with recycled manufactured sand reduced drying shrinkage [9]. This reduction is related to its irregular morphology and coarse texture [10]. Feasibility of using discarded fly ash substituting sand, up to 30%, in cement composites for enhancing technological features and mitigate costs has been examined [11].

Natural pozzolan is extensively utilized in production of building materials, reducing expenses and alleviating green impacts. Pozzolanic materials cannot be employed independently and must solely serve as a partial substitute [12]. Deboucha et al. [13] indicates that the compressive and flexural strengths of mortars with additional NP diminish as NP content and age increase. This may result from diminished pozzolanic reactions between glassy nanoparticle constituents and calcium hydroxide. C-H must be generated through cement hydration prior to the initiation of the pozzolanic reaction. Oviedo et al. [14] found that including pumicite up to 10% as a cement substitute in pervious concrete enhanced its mechanical qualities relative to normal concrete. Al-Amoudi et al. [15] reported that activation of NP with hydrated lime enhanced compressive strength higher than those composed solely out of OPC after 90 days of curing. Numerous research projects have examined the practicality of utilizing other materials to substitute sand for improving qualities. The use of NP and silica fume as a partial replacement for fine aggregate and silica fume respectively enhanced the compressive strengths of mortars, with replacement levels of NP reaching up to 40% and of SF up to 10%, respectively [16]. The use of 20% NP, along with 5% SF, enhanced both tensile and compressive strengths of the concrete by 16.3% and 18%, respectively [17]. Substituting sand with NP with more than 20% diminished both concrete tensile and compressive strengths. Ahmad et al. [18] obtained comparable results, demonstrating that adding 5% SF to a mixture of OPC and 20% NP yielded compressive strengths akin to those of OPC for up to 28 days, after which it surpassed the values of concrete composed of OPC. Fode et al. [33] concluded that investigations revealed that 15% substitution of NP with volcanic sources can provide optimal strength.

Due to possible application of NP, researchers are obligated investigating impact utilizing NP on the properties of cement-based products. It was found that incorporating NP significantly diminishes workability, necessitating using superplasticizers instead of SF [19]. While most studies indicate that NP exhibits pozzolanic activity superior to FA but inferior to SF, and that the optimal dosage of NP ranges from 10 to 20 percent [20], there are inconsistencies regarding the impact of NP on the strength of concrete. Utilizing NP enhances porosity, reduces resistivity, and extends the carbonation front's depth, whereas substituting superfine aggregates diminishes porosity and decreases the carbonation front's depth [21]. Khan and Alhozaimy [22] demonstrated the application of various regional natural pozzolans in Saudi Arabia to produce environmentally sustainable concrete. The researchers discovered a significant presence of NP in Saudi Arabia, which, regardless of its origin, complies with ASTM C618 [23] requirements, it is classified as "Class N" for its characteristics. There is limited research on the effects of NP on the characteristics of concrete with low water/binder ratios (0.3 or below). The intricate behavior of concrete and cement mortars, including diverse supplementary cementitious materials as partial cement substitutes prompted the creation of dependable forecasting models for their mechanical properties.

Various statistical methods were employed for developing predictive models for concrete properties [24,25]. RSM comprises several mathematical and statistical methodologies for the analysis of multiple independent variables effects. RSM can assist in examining the interrelated effects of process elements and in building models that precisely represent

the whole procedure. RSM has been employed in research for experimental design, development of models, and optimization. Employing the Response Surface Methodology (RSM), a series of experiments were conducted to anticipate and enhance the properties of concrete, utilizing rice husk ash as a partial substitute for cement [26–28]. The models show exceptionally precise forecasting concrete properties. Adamu [29] employed Response Surface Methodology for analyzing increased temperature impact on the strength of concrete amended with date palm fiber and silica fume as partial substitutes for cement. Alkharisi and Dahish [30] employed RSM to predict the compressive strength of concrete containing polypropylene fibers, recycled aggregate, and SCMs. Khelifi et al. [31] applied RSM to predict and optimize the physical characteristics of mortars composed of dune sand and Washingtonia waste. Maaroof et al. [32] used RSM with the Genetic Algorithm to predict and optimize compressive strength of cementitious mixtures at various ages based on the chemical compositions.

Zhang et al. [33] utilized RSM for modeling influence of certain SCMs on the properties of cement-based ingredients enhanced by NS. RSM was employed to create predictive models about water-to-cement ratio influence on concrete amended using bentonite [34]. RSM has been employed to examine the impact of integrating calcined bentonite clay into cement mortars [35]. Busari et al. [36] employed RSM to evaluate the impact of integrating metakaolin on the corrosion behavior of reinforcement. Dahish [37] employed RSM to develop predictive models assessing the effects of partially substituting aggregates with crushed rock (CR) and recycled aggregate, on the compressive strength of concrete. Abdulkadir et al. [38] utilized RSM to enhance the mechanical characteristics of high-volume fly ash designed cementitious composite.

This work is aimed at predicting the impact of including NP and SF in cement mortars on compressive strength using RSM. The Central Composite Experimental Design in Response Surface Methodology using Design Expert was employed for evaluating RSM efficacy in forecasting compressive strength of cement mortar with natural pozzolan (NP) as partial replacement for cement and sand and silica fume (SF) as a partial replacement for cement. The experimental data was assessed by fitting them into linear and second-order polynomial models. Models were validated by Analysis of Variance (ANOVA) for assessing significance. Multi-objective optimization for compressive strength of SF-NP mortars is conducted based on optimization framework combining NPC, NPS, and SF. The developed predictive models serve as a predictive tool simulating intricate performance of hardened cement mortars within the specific experimental domain defined by the factor ranges and materials tested.

2. MATERIALS AND METHODS

2.1. Materials

The cement Type I OPC with a specific gravity of 3.15 and the commercially available SF have been used in this research. The utilized NP is sourced from the volcanic region located in western part of Saudi Arabia. Figure 1.a illustrates NP in its unrefined condition utilized as a substitute for sand. Figure 1.b illustrates NP that has been pulverized to finer than 75μ for use as a cement substitute.

(a)

(b)

Fig. 1: Natural pozzolan, (a) coarse; (b) ground.

The model is constructed to match existing two large-scale I-beams experiments (Davalos and Qiao, 1997). The simply supported beam built in the model has a cross section with a flange width and web depth of 12 inches (304.8 mm) and a span of 14.5 feet (4.42 m). The thickness of both the flange and the web is ½ inch (12.7 mm). Since the beams in experiments are stiffened with a wooden stiffener at the mid-span cross-section, the model includes a stiffner at mid-span as shown in Figure 2. The I-beam cross-section is composed of laminates for each of the two flanges and the web in which a perfect bond exists between the top and bottom flanges and the web.

The natural fine aggregate has a specific gravity of 2.6, a water absorption of 0.21%, and a bulk density of 1670 kg/m³. The coarse NP has a specific gravity of 2.51, a water absorption of 5.23%, and a bulk density of 1100 kg/m³. The chemical composition of the used powders is shown in Table 1. The used NP has a total ($SiO_2 + Al_2O_3 + Fe_2O_3$) > 70%, SO_3 < 5%, LOI ≤ 10%) conforming the requirements for Class N natural pozzolans according to ASTM C618 [23]. Figure 2 illustrates the sieve analysis results for the sand and coarse NP.

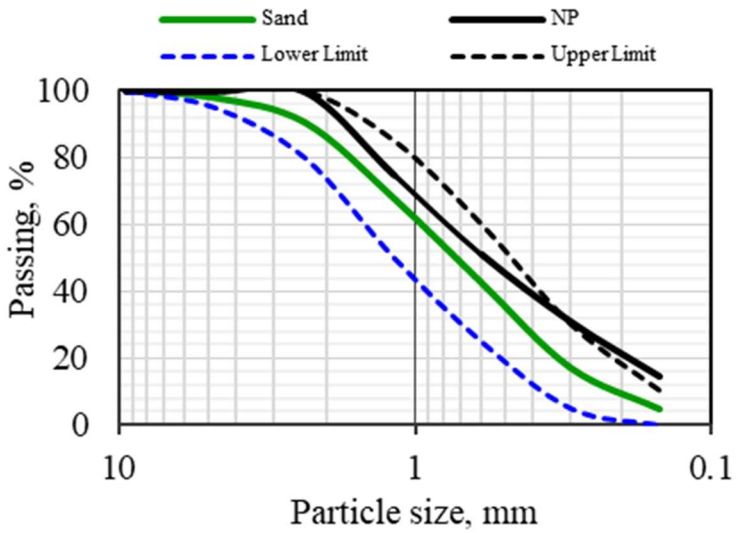

Fig. 2: Gradations of sand and coarse natural pozzolan.

Table 1 Chemical composition of cement, NP, and SF

Oxides	Cement	NP	SF
CaO	64.13	11.21	0.3
Al_2O_3	5.85	15.44	1
SiO_2	19.97	41.12	92
Fe_2O_3	3.43	17.35	1
SO_3	2.8	0.18	0.3
K_2O	0.72	1.05	0.54
MgO	0.6	4.47	0.6
Na_2O	0.16	0.25	0.24
LOI (%)	1.6	2.2	

2.2. Sample preparation

The mortar specimens were prepared by varying the ratios of NP and SF while maintaining a constant water/binder ratio of 0.49. Table 2 shows the control mortar Constituents. For mixing and curing, standard tap water was used. The mixing of mortar ingredients conforms to the standard practice for mechanical mixing of hydraulic cement pastes and mortars of plastic consistency (ASTM C305) [39]. The mortar cube was kept at a temperature of 22 ± 2 °C in water tanks.

The input parameters for the predictive model development included the percentage of NP substituting cement (NPC), the percentage of NP substituting sand (NPS), and the percentage of SF substituting cement (SF). The objective was to predict the compressive strengths of the cement mortars (Fc). Figure 3 illustrates the mortar samples and the compression testing apparatus. The cubic specimens were tested using an automatic concrete compression testing machine with 2000 kN capacity at a loading rate of 1 kN/s conforming ASTM C109 [40]. The compressive strength was calculated as the mean of three test results for each of the twenty mixes after 28 days of curing.

Table 2 Constituents of mortars.

Mix	NPC (%)	SF (%)	NPS (%)	Sand (kg/m^3)	Cement (kg/m^3)	NPC (kg/m^3)	SF (kg/m^3)	NPS (kg/m^3)
1	0	0	0	1480.2	534.9	0	0	0
2	10	0	0	1480.2	481.41	53.49	0	0
3	20	0	0	1480.2	427.92	106.98	0	0
4	30	0	0	1480.2	374.43	160.47	0	0
5	40	0	0	1480.2	320.94	213.96	0	0
6	2.5	2.5	5	1406.2	459.04	13.37	13.37	49.12
7	2.5	5	2.5	1443.2	470.22	13.37	26.75	24.56
8	2.5	7.5	5	1406.2	432.29	13.37	40.12	49.12
9	2.5	5	5	1406.2	445.66	13.37	26.75	49.12
10	2.5	2.5	10	1332.2	409.92	13.37	13.37	98.24
11	2.5	7.5	10	1332.2	383.17	13.37	40.12	98.24
12	0	0	10	1332.2	436.66	0	0	98.24
13	0	0	20	1184.2	338.42	0	0	196.48
14	0	0	30	1036.1	240.18	0	0	294.72
15	0	0	40	888.1	141.94	0	0	392.96
16	0	5	10	1332.2	409.91	0	26.75	98.24
17	0	5	20	1184.2	311.67	0	26.75	196.48
18	0	5	30	1036.1	213.43	0	26.75	294.72
19	0	5	40	888.1	115.19	0	26.75	392.96
20	0	10	10	1332.2	383.17	0	53.49	98.24
21	0	10	20	1184.2	284.93	0	53.49	196.48
22	0	10	30	1036.1	186.69	0	53.49	294.72
23	0	10	40	888.1	88.45	0	53.49	392.96

Fig. 3: (a) sample of cement mortar, (b) compression test.

2.3. Regression Model

RSM is an advanced tool that uses various types of statistical and mathematical methodologies to conceptualize, simulate, assess, create, and enhance optimization processes. It has demonstrated efficacy as a methodology for multi-objective optimization by delineating the desired objectives for output and inputs [41,42]. The quantity of variable levels and the characteristics of the accessible data determine the model employed. The user-defined parameters can be utilized for model construction and analysis inside a previously established experiment matrix. Linear or higher-degree polynomials may be employed to establish a correlation between the independent variables and the answers. Equation (1) represents the generalized linear relationship between output and input variables. Equation (2) represents the second order or higher polynomials relationship between output and input variables.

$$Y = r_o + r_1X_1 + r_2X_2 + \cdots r_nX_n + \theta \quad (1)$$

$$Y = r_o + \sum_{i=1}^{n} r_iX_i + \sum_{i=1}^{n} r_{ii}\,X_j^2 + \sum_{i<}\sum_{j}\; r_{ij}\,X_iX_j + \theta \quad (2)$$

Where Y is the response variable; r_o is a constant; r_i is the linear term coefficient; r_{ij} is the interaction term coefficient; r_{ii} is the second-order term coefficient; X_i, X_j are the process variables; n is the number of process variables; θ is a random error.

RSM consists of three primary segments. Initially, conduct the experimental approach multiple times utilizing varying parameter values. Secondly, employ regression modeling to establish a suitable interaction between the response and the input variables. Ultimately, optimization is employed to ascertain the influence of each parameter on the result [43]. The Design Expert software, proficient in optimizing intricate systems for scientific applications, was employed to assess the experimental data [44,45].

3. RESULTS AND DISCUSSIONS

3.1. Compressive strength results

Figure 4 illustrates the compressive strength (CS) of mortar cubes after 28 days, incorporating varied quantities of NP powder as a substitute for cement. Substituting cement at levels of 10%, 20%, 30%, and 40% with NP powder resulted in a reduction of mortar compressive strengths at 28 days. The decrease in strength is chiefly attributable to the sluggish reactivity of the NP during first stages. The 28-day compressive strengths (Fc) were 45.11 MPa, 39.6 MPa, 37.46 MPa, 28.54 MPa, and 21.14 MPa for mortars with 0, 10%, 20%, 30%, and 40% NPC, respectively. The replacement of cement with NPC at levels of 10%, 20%, 30%, and 40% led to reductions in the Fc by 12.2%, 17%, 36.7%, and 53.1%, respectively.

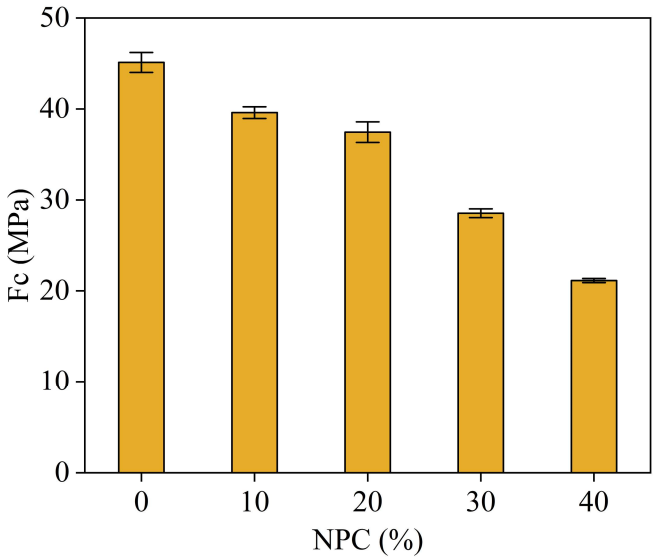

Fig. 4: Compressive strengths of NPC-mortars.

Figure 5 illustrates the variation in compressive strength of mortar cubes after 28 days, contingent upon varying proportions of substituting sand with NP and cement with SF. Substituting sand with 20% NP improved CS. The physical characteristics of used NP in their coarse form (rough surface roughness) improve the adhesion between cement paste and aggregate, hence augmenting strength. Suboptimal particle coating and insufficient reactivity at fixed cement amounts may diminish strength at elevated levels of NP. Silica fume enhances Fc of NP-mortars. The replacement level of NP with NPS up to 20% without SF improved the compressive strength. The presence of 5% SF as cement partial replacement improved Fc for mortars containing NPC up to 30%. The inclusion of 10% SF as cement partial replacement improved Fc for mortars containing NPC up to 40%.

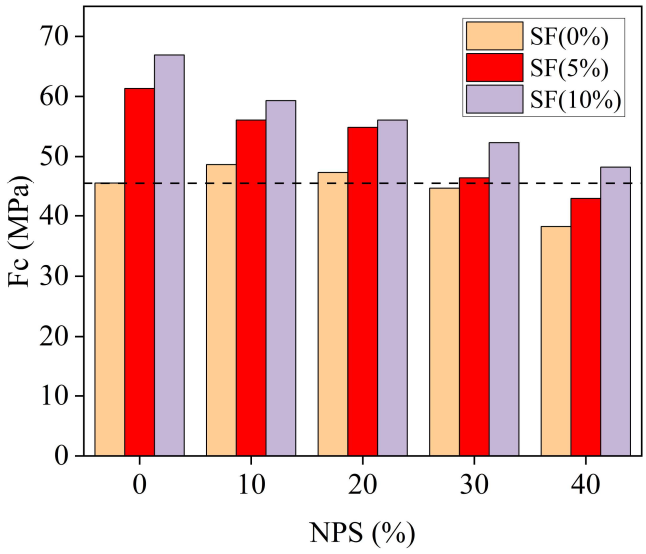

Fig. 5: Compressive strengths of NPS mortars.

3.2. Dataset statistics

This study used a dataset of 23 mixes of compressive strength test results for cement mortars containing NP and SF. The dataset offers a thorough experimental analysis of natural pozzolan (NP) in concrete. The summary of data statistics is shown in Table 3. The independent variable, NP as cement replacement (NPC), demonstrates a pronounced right-skewed distribution (skewness = 2.213), signifying that most mixtures had minimal to no NPC (mean = 4.85%), although a specific sample investigated elevated replacement levels reaching up to 40%. In contrast, the distributions for silica fume (SF) and natural pozzolan as sand (NPS) exhibit relative flatness and uniformity (negative kurtosis), affirming their systematic variation within their respective ranges (0-10% and 0-40%). The response variable, compressive strength (Fc), exhibits a broad performance range (20.9-63.6 MPa) with a small left skew with a mean of 46.89 MPa.

Table 3: Dataset statistics' summary.

	Unit	Minimum	Maximum	Std. Deviation	Mean	Kurtosis	Skewness
NP as cement (NPC)	%	0	40	11.13	4.85	3.637	2.213
Silica fume (SF)	%	0	10	4.09	3.75	-1.325	0.497
NP as sand (NPS)	%	0	40	15.1	14.71	-1.271	0.486
Compressive Strength (Fc)	MPa	20.9	63.6	10.46	46.89	0.318	-0.712

3.3. Correlation between input and output parameters

Figure 6 illustrates the relationship between the input parameters and compressive strength (Fc), highlighting the varied effects of each material. The replacement of cement with natural pozzolan (NPC) exhibits a strong negative correlation with Fc, indicating that increasing the NP content as a cement substitute is generally associated with a reduction in compressive strength. The partial substitution of sand with natural pozzolan (NPS) has a little or negligible correlation with strength, indicating that this replacement approach, within the examined parameters, has a minimal effect on mechanical performance. The inclusion of silica fume (SF) exhibits a moderate positive correlation with Fc, underscoring its efficacy as a pozzolanic additive that might reduce strength deterioration and possibly boost performance.

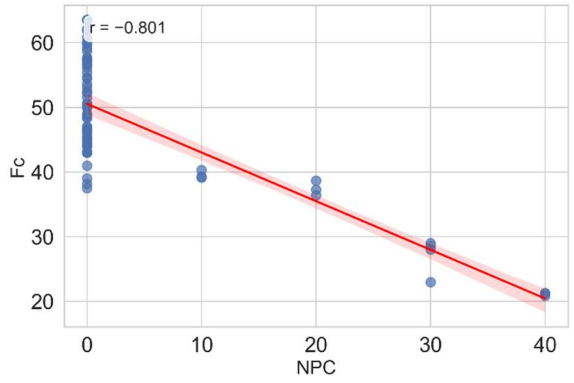

(a)

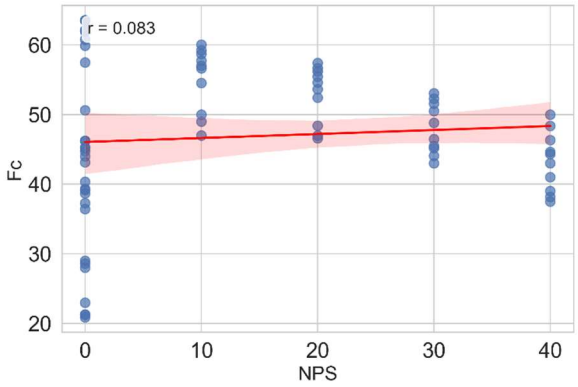

(b)

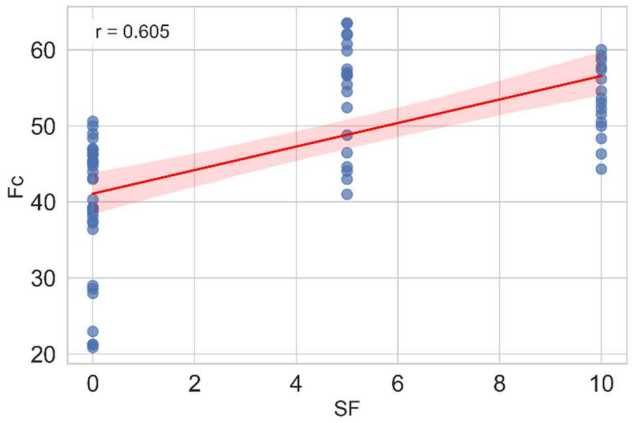

(c)

Fig. 6: Relation between input and output parameters.

3.4. Analysis of Variance (ANOVA)

The ANOVA summary shown in Table 4 indicates that the input parameters: NPC, SF, and NPS, significantly affect compressive strength (Fc) in both linear and quadratic models with p-value less than 0.0001). A typical stepwise regression with backward elimination based on p-values < 0.05 to choose the model terms was employed. This removed variables that are not statistically significant to the model. In the linear model, all variables exhibited significant individual predictors with p-value < 0.0001. The quadratic model, which includes interaction and squared factors, shows a significantly enhanced fit, as indicated by a considerable decrease in the residual sum of squares. The notable interaction term SF□NPS and the quadratic terms SF^2 and NPS^2 indicate critical non-linear and synergistic correlation among the predictors, especially with silica fume and sand replacement. The lack of fit results shows that neither model shows a lot of unexplained systematic variance beyond experimental error. The linear model's lack of fit F-value is 1.3023, with a p-value of 0.23, which is much higher than 0.05. The quadratic model has a lower lack of fit with an F-value of 0.556 and a p-value of 0.85, showing that adding interaction and curvature components made the residual variance more like pure noise. Statistically, both models suit the data structure well.

The results of statistical tests for Fc models, as shown in Table 5, demonstrate a considerable enhancement in predictions from the linear to the quadratic model. The linear model has an R^2 value of 0.8959 and an adequate precision of 46.95, although it presents a coefficient of variation (C.V.) of 7.36% and a standard deviation of 3.45, signifying substantial prediction error. The substantial enhancement achieved by quadratic and interaction variables is evidenced by the quadratic model's superior metrics: a decrease in standard deviation to 2.57 and C.V. to 5.49%, along with an increase in R^2 to 0.9449. The high and closely values of adjusted R^2 (0.9395) and predicted R^2 (0.9321) signify a superior generalization of the underlying data structure.

The developed prediction equations for predicting Fc are shown in Equations 1 and 2. The linear model (Equation 3) allocates a negative coefficient to both natural pozzolan substitutes, exhibiting a more adverse impact for NPC (-0.76) in contrast to NPS (-0.32), whilst silica fume (SF) demonstrates a favorable effect (+1.21). Conversely, the quadratic model (Equation 4) provides a more sophisticated and accurate interpretation, commencing from a reduced baseline of 47.63 MPa. It substantiates the predominant adverse impact of NPC (-0.66) while disclosing significant non-linearities for the other variables: the influence of SF is not only markedly positive (+2.87) but also experiences diminishing returns (indicated by the negative SF^2 term), whereas the contribution of NPS is minimal as a linear main effect (-0.023) yet demonstrates a slight curvilinear correlation. The model notably reveals a substantial synergistic interaction via the

positive SF×NPS term, signifying that the concurrent utilization of silica fume and natural pozzolan as sand substitutes yields a sub-additive effect on strength.

$$Fc = 50.78592 - 0.760577NPC + 1.21087SF - 0.322468NPS \quad (3)$$

$$Fc = 47.63135 - 0.655424NPC + 2.87188SF - 0.023298NPS + 0.025723SF{\times}NPS - 0.123211SF^2 - 0.004859NPS^2 \quad (4)$$

where *Fc* is the compressive strength; *NPC* is the percentage of NP replacing cement; *NPS* is the percentage of NP replacing sand; and *SF* is the percentage of silica fume replacing cement.

Table 4: ANOVA summary.

Model	**Source**	**Sum of Squares**	**df**	**Mean Square**	**F-value**	**p-value**	
Linear model	Model	6563.44	3	2187.81	183.62	< 0.0001	significant
	A-NPC	3616.61	1	3616.61	303.54	< 0.0001	
	B-SF	1245.75	1	1245.75	104.56	< 0.0001	
	C-NPS	1178.01	1	1178.01	98.87	< 0.0001	
	Residual	225.7	64	3.53			
	Lack of Fit	60.31	14	4.3	1.3023	0.23	Not significant
	Pure Error	165.39	50	3.31			
	Cor Total	7325.98	67				
Quadratic model	Model	6922.36	6	1153.73	174.36	< 0.0001	significant
	A-NPC	2239.89	1	2239.89	338.51	< 0.0001	
	B-SF	978.17	1	978.17	147.83	< 0.0001	
	C-NPS	1190.74	1	1190.74	179.96	< 0.0001	
	BC	87.48	1	87.48	13.22	0.0006	
	B^2	103.55	1	103.55	15.65	0.0002	
	C^2	30.55	1	30.55	4.62	0.0356	
	Residual	185.63	61	3.04			
	Lack of Fit	20.24	11	1.84	0.556	0.85	Not significant
	Pure Error	165.39	50	3.31			
	Cor Total	7325.98	67				

Table 5: Statistical tests of Fc responses

Model	**Adequate Precision**	**R^2**	**Adjusted R^2**	**Predicted R^2**	**Std. Dev.**	**Mean**	**C.V. %**
Linear	46.9518	0.8959	0.891	0.8847	3.45	46.89	7.36
Quadratic	47.6467	0.9449	0.9395	0.9321	2.57	46.89	5.49

3.5. Diagnostic Plots

The residuals vs run number graphs shown in Figure 7 offer a crucial diagnostic evaluation of the temporal stability and independence of errors in the models created for predicting the compressive strength (Fc) of NP-mortars. The externally studentized residuals for both Model 1 (linear) and Model 2 (quadratic) are displayed against the order of experimental runs, indicating the sequence of data collection. In all panels, the residuals are symmetrically distributed around the zero line, exhibiting no identifiable systematic pattern, trend, or clustering during the run sequence. This indicates that errors are randomly distributed and lack autocorrelation or temporal pattern, thereby reinforcing the premise of independence across observations. The lack of funnel-shaped patterns or variations in variability with run number further signifies the homogeneity of variance (homoscedasticity) throughout the experimental timeframe. All residuals are contained within the approximate limits of ±3.56, with none surpassing the conventional critical criteria that would indicate significant outliers. This indicates that both models effectively represent the fundamental relationship without systematic bias from the testing sequence. Figure 7 substantiates the robustness of the Fc modeling process concerning run order, and the residuals exhibit behavior aligned with the fundamental assumptions of regression analysis, hence enhancing the trustworthiness of the statistical inferences derived from both models.

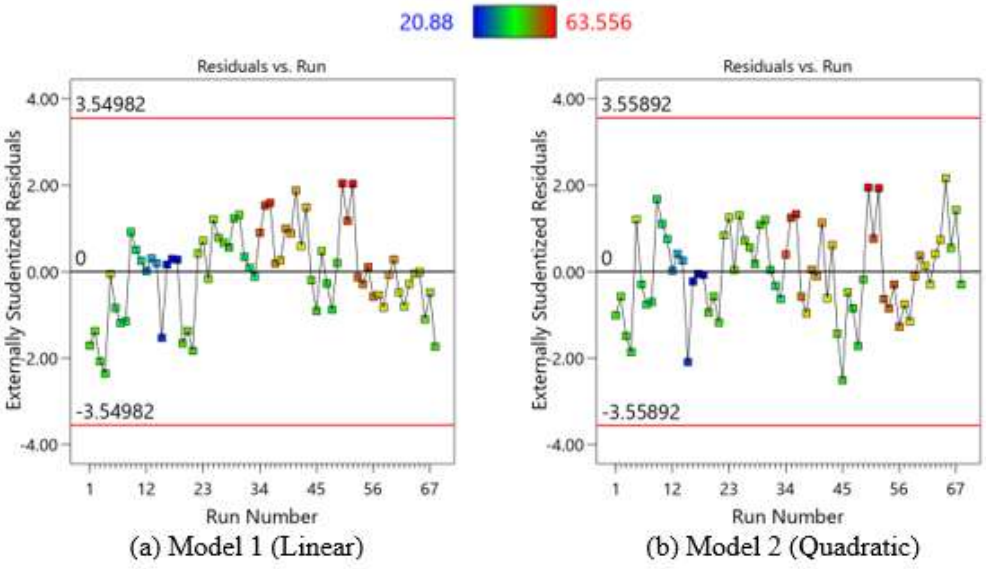

Fig. 7: Residuals vs run number plots.

Figure 8 illustrates the experimental values compared to the predicted values for the compressive strength (Fc) of NP-mortars, providing a visual evaluation of model accuracy and predictive efficacy. The extent of dispersion around this optimal line measures the prediction error; a compact cluster of points indicates that the model accounts for a significant percentage of the variance in the experimental data, with negligible residual error. In contrast, extensive, diffuse scattering indicates much unexplained variability. The analysis of this figure necessitates assessing the symmetrical distribution of points relative to the line throughout the complete spectrum of compressive strengths, which would signify that the model's accuracy is uniform and not skewed towards either low or high strength values. The lack of systematic curvature or pattern in the deviations validate the appropriateness of the model's predictions. The models are both statistically valid and practically applicable for predicting the compressive strength of NP-mortars based on the specified input parameters.

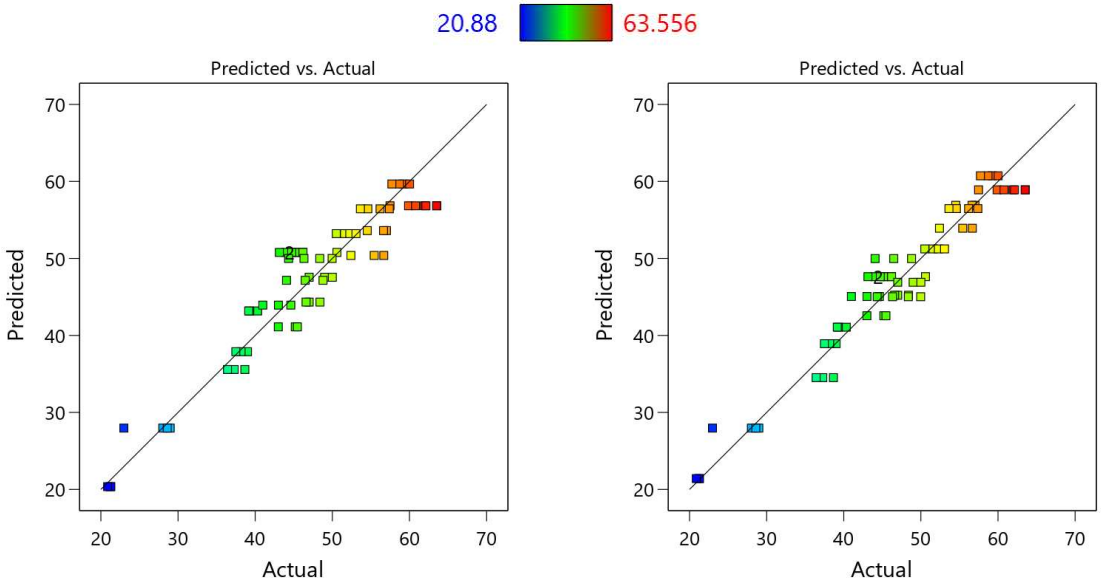

(a) Model 1 (Linear) (b) Model 2 (Quadratic)

Fig. 8: Experimental values vs predictions.

Figure 8 illustrates the experimental values compared to the predicted values for the compressive strength (Fc) of NP-mortars, providing a visual evaluation of model accuracy and predictive efficacy. The extent of dispersion around this optimal line measures the prediction error; a compact cluster of points indicates that the model accounts for a significant percentage of the variance in the experimental data, with negligible residual error. In contrast, extensive, diffuse scattering indicates much unexplained variability. The analysis of this figure necessitates assessing the symmetrical distribution of points relative to the line throughout the complete spectrum of compressive strengths, which would signify that the model's accuracy is uniform and not skewed towards either low or high strength values. The lack of systematic curvature or pattern in the deviations validate the appropriateness of the model's predictions. The models are both statistically valid and practically applicable for predicting the compressive strength of NP-mortars based on the specified input parameters.

3.6. Response Surface Plots

Figure 9 illustrates the 2D contour plots and 3D response surface plots depicting the synergistic effects of NPC, NPS, and SF on the compressive strength (Fc) of NP-mortars as forecasted by the quadratic model. The results demonstrate that Fc is acutely responsive to both the individual impacts of these components and their interaction effects, as indicated by the anticipated values. The seamless and continuous characteristics of the response surfaces validate the nonlinear dynamics of the system and the suitability of the constructed model in representing these interactions.

The synergistic impact of NPS and SF on Fc (Figure 9a) indicates that SF significantly enhances compressive strength, while NPS generally has a detrimental effect, especially at elevated replacement levels. Augmenting the SF content significantly improves Fc throughout the whole NPS spectrum, with peak strengths achieved at elevated SF levels (10%) and reduced NPS values (≤10%). A steady decrease in Fc is found at high NPS levels, particularly when SF is low. This pattern indicates that while small quantities of NPS may enhance particle packing, excessive NPS likely elevates water demand, leading to a compromised cementitious matrix. The advantageous function of SF is due to its significant pozzolanic reactivity and micro-filling capacity, which enhance the pore structure and somewhat mitigate the negative impacts of NPS.

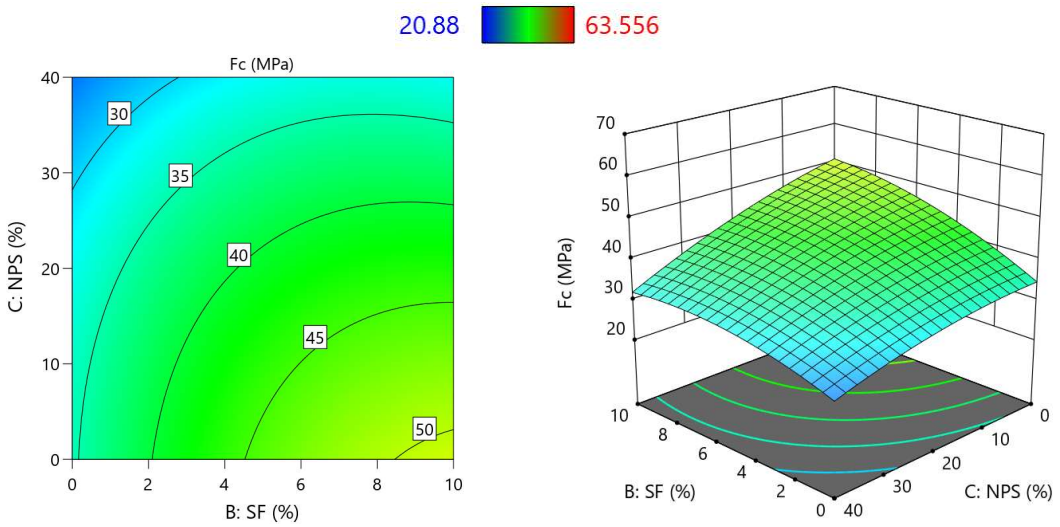

(a) Effect of NPS and SF on CS

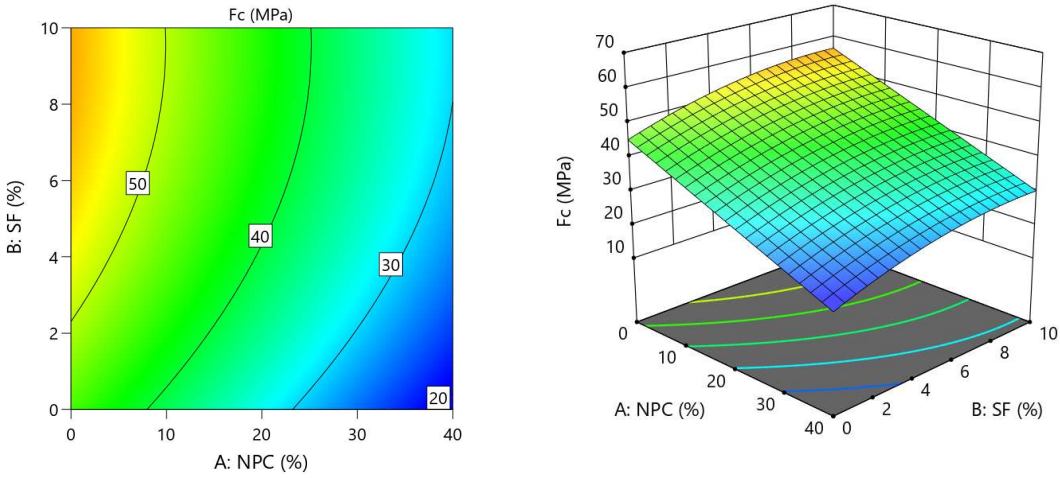

(b) Effect of NPC and SF on CS

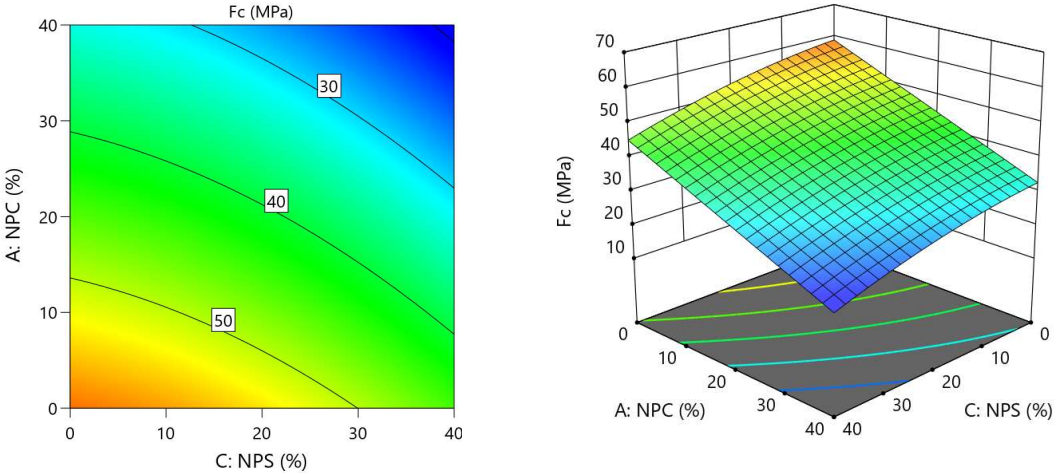

(c) Effect of NPC and NPS on CS

Fig. 9: 2D and 3D plots for NP-mortar compressive strength (Model 2)

Figure 9b depicts the relationship between NPC and SF. A discernible reduction in Fc is noted with escalating NPC content, signifying that elevated cement replacement adversely impacts compressive strength. This drop is ascribed to cement dilution and the resulting reduction in hydration products. In contrast, augmenting SF material consistently enhances Fc across all NPC levels. Nonetheless, the reinforcing impact of SF diminishes with elevated NPC concentrations. Optimal compressive strengths are attained at low NPC levels (≤10%) in conjunction with elevated SF concentrations (≥7–10%).

Figure 9c illustrates the synergistic impact of NPC and NPS on Fc. Both factors exhibit a deleterious effect on compressive strength when elevated concurrently, culminating in the lowest Fc values in the high-NPC/high-NPS area. This behavior underscores the lack of synergy between NPC and NPS at high concentrations. The decline in strength may be linked to high fine content, which hinders proper particle packing, elevates porosity, and compromises the interfacial transition zones. The region of maximum strength is associated with low NPC and low NPS levels, highlighting the necessity of restricting total NP replacement in NP-mortars.

The results indicate that SF is the primary factor in improving the compressive strength of NP-mortars, although both NPC and NPS require meticulous optimization. Excessive substitution levels of either NP component, especially when combined, substantially undermine strength. The results indicate that optimal NP-mortar performance is attained via a balanced mix design featuring elevated SF content and low to moderate levels of NPC and NPS. These results offer essential insights for the sustainable design of NP-modified mortars, necessitating a simultaneous consideration of material efficiency and mechanical performance.

3.7. Optimization Results

The optimization outcomes for the compressive strength (Fc) of NP-mortars, derived from the quadratic model and a desirability-based methodology, are illustrated in Figure 10. The aim of the optimization was to enhance Fc by determining the ideal combination of NPC, SF, and NPS within the examined design space.

Case 1 shown in Figure 10(a) achieved the maximum predicted compressive strength (Fc) of 56.833 MPa by maximizing NPC at around 11% and using 10% SF content. This implies that the primary driver for strength maximization under these limits is the synergistic combination of moderate NPC and high SF. The relatively high desirability of 0.699 indicates that this is a powerful, feasible approach for pure strength maximization.

Case 2 shown in Figure 10(b), which maximizes NPS and Fc while setting NPC and SF in their ranges, produces a much different optimum point. The greatest strength of 53.641 MPa under this constraint is reached with a high NPS at around 26% and a moderate SF content at around 9%. This finding is especially interesting since it shows that extensive sand replacement with natural pozzolan might be useful for strength growth. The high desirability of 0.731 among the scenarios shows that this scenario strikes a good compromise between optimizing strength and incorporating a large volume of natural pozzolan into the sand fraction.

Case 3 shown in Figure 10(c), which maximizes both NPC and NPS along with Fc, yields the lowest expected strength of 52.466 MPa and a desirability of 0.571. The solution provides moderate levels of NPC at around 9.6% and NPS at around 14.9% with maximal SF. This demonstrates a clear antagonistic interaction between NPC and NPS; attempting to maximize both concurrently reduces the overall strength potential, most likely due to an excessive reduction in effective binder content or increased water demand that is not fully compensated for in the model's fixed w/b ratio framework.

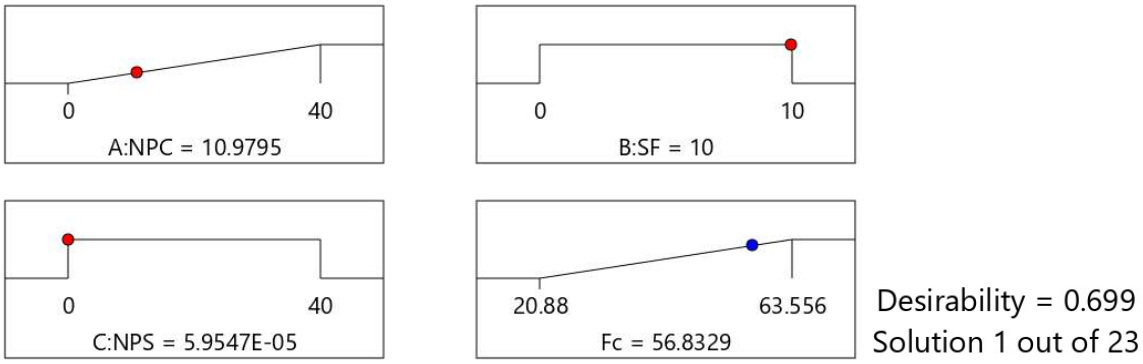

(a)

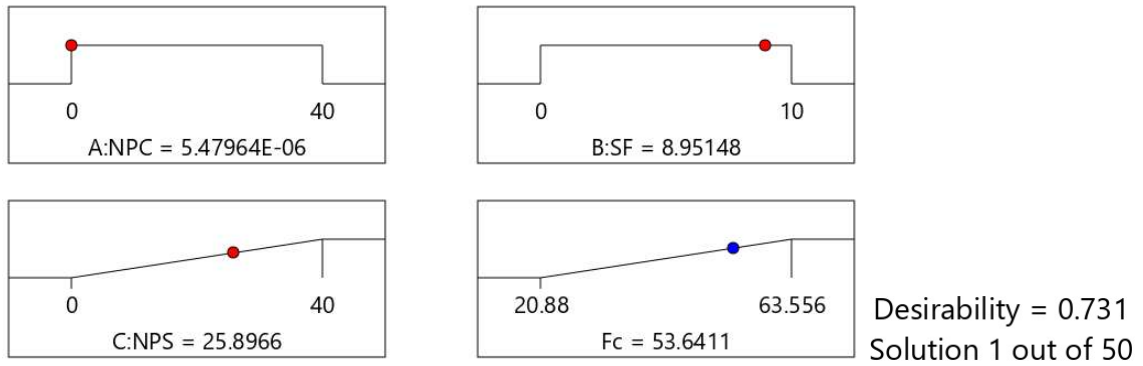

(b)

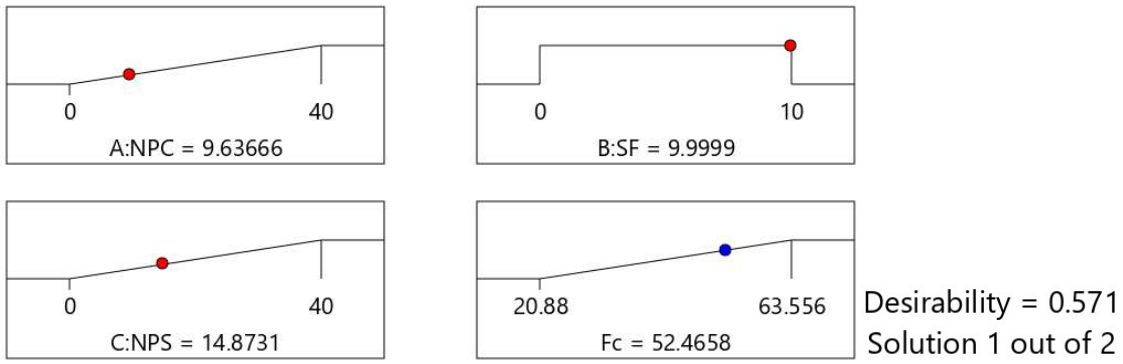

(c)

Fig. 10: Optimal NP-mortar compressive strength without NPC (Quadratic model).

4. CONCLUSIONS

This study examined the impact of including NP and SF in cement mortars on compressive strength using RSM. Two models employing linear and nonlinear regression were created. The subsequent findings were derived:

- At 28 days, the compressive strengths of the mortar diminished when cement was substituted with NP powder at all replacement ratios. The delayed NP response in the initial phases leads to a decline in mechanical strength.
- Sand containing 20% NP enhanced compressive strength. The rough surface texture of NP enhances the adhesion between aggregate and cement paste, hence augmenting strength.
- SF enhanced the compressive strength of NP-mortars across all replacement ratios.
- RSM was employed to develop the prediction models for Fc of NP-mortar with a strong correlation and an error margin of less than 5%.
- All created models had p-values below 0.05, indicating a strong connection for predictive accuracy. The R^2 for the quadratic model exceeds 90%, signifying a substantial correlation and its applicability in forecasting the compressive strength of NP-mortars.
- The optimal mix for peak strength (56.8 MPa, desirability 0.699) is 11% NPC and 10% SF. The best mix for high-volume use of NPS (53.6 MPa, desirability 0.731) is around 26% NPS and 9% SF. Combining both NPC and NPS (9.6% NPC, 14.9% NPS) lowers strength to 52.5 MPa, which shows that the individual replacement is more effective than the dual replacement.

Future research should include multi-age testing (7, 28, 56, and 90 days) to comprehensively model and elucidate the progressive pozzolanic contribution of NP over time.

REFERENCES

[1] O.E. Ige, O.A. Olanrewaju, K.J. Duffy, O.C. Collins, Environmental Impact Analysis of Portland Cement (CEM1) Using the Midpoint Method, Energies (Basel) 15 (2022) 2708. https://doi.org/10.3390/en15072708.

[2] A. Bărbulescu, K. Hosen, Cement Industry Pollution and Its Impact on the Environment and Population Health: A Review, Toxics 13 (2025) 587. https://doi.org/10.3390/toxics13070587.

[3] M.C.G. Juenger, R. Siddique, Recent advances in understanding the role of supplementary cementitious materials in concrete, Cem Concr Res 78 (2015) 71–80. https://doi.org/10.1016/j.cemconres.2015.03.018.

[4] S.U. Khan, M.F. Nuruddin, T. Ayub, N. Shafiq, Effects of Different Mineral Admixtures on the Properties of Fresh Concrete, The Scientific World Journal 2014 (2014) 1–11. https://doi.org/10.1155/2014/986567.

[5] B. Pacewska, I. Wilińska, Usage of supplementary cementitious materials: advantages and limitations, J Therm Anal Calorim 142 (2020) 371–393. https://doi.org/10.1007/s10973-020-09907-1.

[6] W. Zhuang, S. Li, Q. Yu, The effect of supplementary cementitious material systems on dynamic compressive properties of ultra-high performance concrete paste, Constr Build Mater 321 (2022) 126361. https://doi.org/10.1016/j.conbuildmat.2022.126361.

[7] H.X. Li, Effects of Silica Fume on Concrete Compressive Strength, Applied Mechanics and Materials 744–746 (2015) 78–81. https://doi.org/10.4028/www.scientific.net/AMM.744-746.78.

[8] A.B. Padavala, M. Potharaju, V.R. Kode, Mechanical properties of ternary blended mix concrete of fly ash and silica fume, Mater Today Proc 43 (2021) 2198–2202. https://doi.org/10.1016/j.matpr.2020.12.127.

[9] M.A. Nawaz, B. Ali, L.A. Qureshi, H.M. Usman Aslam, I. Hussain, B. Masood, S.S. Raza, Effect of sulfate activator on mechanical and durability properties of concrete incorporating low calcium fly ash, Case Studies in Construction Materials 13 (2020) e00407–e00407. https://doi.org/10.1016/j.cscm.2020.e00407.

[10] Z. Ma, J. Shen, C. Wang, H. Wu, Characterization of sustainable mortar containing high-quality recycled manufactured sand crushed from recycled coarse aggregate, Cem Concr Compos 132 (2022) 104629. https://doi.org/10.1016/j.cemconcomp.2022.104629.

[11] J. Harasymiuk, A. Rudziński, Old Dumped Fly Ash as a Sand Replacement in Cement Composites, Buildings 10 (2020) 67. https://doi.org/10.3390/buildings10040067.
[12] S.M.Q. Taklymi, O. Rezaifar, M. Gholhaki, Investigating the properties of bentonite and kaolin modified concrete as a partial substitute to cement, SN Appl Sci 2 (2020) 2023. https://doi.org/10.1007/s42452-020-03380-z.
[13] W. Deboucha, N. Leklou, A. Khelidj, M.N. Oudjit, Natural pozzolana addition effect on compressive strength and capillary water absorption of Mortar, Energy Procedia 139 (2017) 689–695. https://doi.org/10.1016/j.egypro.2017.11.273.
[14] I. Oviedo, M. Pradena, Ó. Link, J.T. Balbo, Using Natural Pozzolans to Partially Replace Cement in Pervious Concretes: A Sustainable Alternative?, Sustainability 14 (2022) 14122. https://doi.org/10.3390/su142114122.
[15] O.S. Baghabra Al-Amoudi, S. Ahmad, M. Maslehuddin, S.M.S. Khan, Lime-activation of natural pozzolan for use as supplementary cementitious material in concrete, Ain Shams Engineering Journal 13 (2022) 101602. https://doi.org/10.1016/j.asej.2021.09.029.
[16] H.A. Dahish, S. Almutairi, A.F. Elragi, S.M. Elkholy, Utilizing Local Natural Pozzolan as Partial Replacement for Cement and Sand in Cement Mortar Cubes with Silica Fume, ARPN Journal of Engineering and Applied Sciences 15 (2020) 1602–1611. https://www.arpnjournals.org/jeas/research_papers/rp_2020/jeas_0820_8269.pdf.
[17] H.A. Dahish, S. Almutairi, Partial Replacement of Sand in Concrete with Available Natural Pozzolan in KSA, International Review of Civil Engineering 13 (2022) 137–145. https://doi.org/10.15866/irece.v13i2.20037.
[18] S. Ahmad, O.S. Baghabra Al-Amoudi, S.M.S. Khan, M. Maslehuddin, Effect of silica fume inclusion on the strength, shrinkage and durability characteristics of natural pozzolan-based cement concrete, Case Studies in Construction Materials 17 (2022) e01255–e01255. https://doi.org/10.1016/j.cscm.2022.e01255.
[19] M. Valipour, F. Pargar, M. Shekarchi, S. Khani, Comparing a natural pozzolan, zeolite, to metakaolin and silica fume in terms of their effect on the durability characteristics of concrete: A laboratory study, Constr Build Mater 41 (2013) 879–888. https://doi.org/10.1016/j.conbuildmat.2012.11.054.
[20] S. Choucha, A. Benyahia, M. Ghrici, M.S. Mansour, Effect of natural pozzolan content on the properties of engineered cementitious composites as repair material, Frontiers of Structural and Civil Engineering 12 (2018) 261–269. https://doi.org/10.1007/s11709-017-0394-x.
[21] J.J. Santana, N. Rodríguez-Brito, C. Blanco-Peñalver, V.F. Mena, R.M. Souto, Durability of Reinforced Concrete with Additions of Natural Pozzolans of Volcanic Origin, Materials 15 (2022) 8352. https://doi.org/10.3390/ma15238352.
[22] M.I. Khan, A.M. Alhozaimy, Properties of natural pozzolan and its potential utilization in environmental friendly concrete, Canadian Journal of Civil Engineering 38 (2011) 71–78. https://doi.org/10.1139/L10-112.
[23] ASTM C618-22, Standard Specification for Coal Fly Ash and Raw or Calcined Natural Pozzolan for Use in Concrete, ASTM International: West Conshohocken, PA, USA (2022).
[24] H. Imran, N.M. Al-Abdaly, M.H. Shamsa, A. Shatnawi, M. Ibrahim, K.A. Ostrowski, Development of Prediction Model to Predict the CompressiveStrength of Eco-Friendly Concrete Using MultivariatePolynomial Regression Combined with Stepwise Method, Materials 15 (2022). https://doi.org/10.3390/ma15010317.
[25] U.K. Unamba, E.S. Nwajagu, J. Abutu, O.J. Agbo-Anike, Predictive Model of the Compressive Strength of Concrete Containing Coconut Shell Ash as Partial Replacement of Cement Using Multiple Regression Analysis, 2021. www.ijisrt.com600.
[26] M. Adamu, K.O. Ayeni, S.I. Haruna, Y.E.H. Ibrahim Mansour, S. Haruna, Durability performance of pervious concrete containing rice husk ash and calcium carbide: A response surface methodology approach, Case Studies in Construction Materials 14 (2021). https://doi.org/10.1016/j.cscm.2021.e00547.
[27] M. Haque, S. Ray, A.F. Mita, S. Bhattacharjee, M.J. bin Shams, Prediction and optimization of the fresh and hardened properties of concrete containing rice hush ash and glass fiber using response surface methodology, Case Studies in Construction Materials 14 (2021). https://doi.org/10.1016/j.cscm.2021.e00505.
[28] K.A. Buyondo, P.W. Olupot, J.B. Kirabira, A.A. Yusuf, Optimization of production parameters for rice husk ash-based geopolymer cement using response surface methodology, Case Studies in Construction Materials 13 (2020). https://doi.org/10.1016/j.cscm.2020.e00461.

[29] M. Adamu, Y.E. Ibrahim, H. Alanazi, Evaluating the Influence of Elevated Temperature on Compressive Strength of Date-Palm-Fiber-Reinforced Concrete Using Response Surface Methodology, Materials 15 (2022). https://doi.org/10.3390/ma15228129.

[30] M.K. Alkharisi, H.A. Dahish, The Application of Response Surface Methodology and Machine Learning for Predicting the Compressive Strength of Recycled Aggregate Concrete Containing Polypropylene Fibers and Supplementary Cementitious Materials, Sustainability 17 (2025) 2913. https://doi.org/10.3390/su17072913.

[31] A. Khelifi, M. Boumaaza, A. Belaadi, M. Bourchak, T. Djedid, I.M.H. Alshaikh, D. Ghernaout, RSM approach-based analysis of the physical behavior of dune sand reinforced with Washingtonia waste contributing to mortar cleaner production, Case Studies in Construction Materials 22 (2025) e04335. https://doi.org/10.1016/j.cscm.2025.e04335.

[32] R.S. Maaroof, A.S. Hamad, M.M.F. Hussein, A novel hybrid metaheuristic algorithm and response surface methodology approach for predictive modeling and optimization of cementitious compressive strength, Sci Rep (2025). https://doi.org/10.1038/s41598-025-32836-8.

[33] X. Zhang, L. Lin, M. Bi, H. Sun, H. Chen, Q. Li, R. Mu, Multi-Objective Optimization of Nano-Silica Modified Cement-Based Materials Mixed With Supplementary Cementitious Materials Based on Response Surface Method, Front Mater 8 (2021). https://doi.org/10.3389/fmats.2021.712551.

[34] M.A.K. Reddy, V.R. Rao, K.N. Chaitanya, V.K.C. Khed, Optimization of Bentocrete parameters using Response Surface Methodology (RSM), AIMS Mater Sci 8 (2021) 221–246. https://doi.org/10.3934/matersci.2021015.

[35] S.S. Reddy, M.A.K. Reddy, Optimization of calcined bentonite caly utilization in cement mortar using response surface methodology, International Journal of Engineering, Transactions A: Basics 34 (2021) 1623–1631. https://doi.org/10.5829/IJE.2021.34.07A.07.

[36] A.A. Busari, W.K. Kupolati, J.M. Ndambuki, E.R. Sadiku, J. Snyman, L. Tolulope, O. Keren, A. Oluwaseun, Response Surface Analysis of the Corrosion Effect of Metakaolin in Reinforced Concrete, Silicon 13 (2021) 2053–2061. https://doi.org/10.1007/s12633-020-00587-y.

[37] H.A. Dahish, Predicting the compressive strength of concrete containing crumb rubber and recycled aggregate using response surface methodology, International Journal of GEOMATE 24 (2023). https://doi.org/10.21660/2023.104.3788.

[38] I. Abdulkadir, B.S. Mohammed, M.S. Liew, M.M.A. Wahab, Modelling and multi-objective optimization of the fresh and mechanical properties of self-compacting high volume fly ash ECC (HVFA-ECC) using response surface methodology (RSM), Case Studies in Construction Materials 14 (2021). https://doi.org/10.1016/j.cscm.2021.e00525.

[39] ASTM C305-20, Standard Practice for Mechanical Mixing of Hydraulic Cement Pastes and Mortars of Plastic Consistency, ASTM International: West Conshohocken, PA, USA (2020).

[40] ASTM C109/C109M-20b, Test Method for Compressive Strength of Hydraulic Cement Mortars, ASTM International: West Conshohocken, PA, USA (2020).

[41] D.C. Montgomery, Design and analysis of experiments, 10th ed., 2019.

[42] M. Adamu, S.I. Haruna, Y.E. Ibrahim, H. Alanazi, Evaluation of the mechanical performance of concrete containing calcium carbide residue and nano silica using response surface methodology, Environmental Science and Pollution Research 29 (2022) 67076–67102. https://doi.org/10.1007/s11356-022-20546-x.

[43] E. Kilickap, M. Huseyinoglu, A. Yardimeden, Optimization of drilling parameters on surface roughness in drilling of AISI 1045 using response surface methodology and genetic algorithm, International Journal of Advanced Manufacturing Technology 52 (2011) 79–88. https://doi.org/10.1007/s00170-010-2710-7.

[44] T.D. Munusamy, S.Y. Chin, Md.M. Rahman Khan, Photoreforming hydrogen production by carbon doped exfoliated g-C3N4: Optimization using design expert®software, Mater Today Proc 57 (2022) 1162–1168. https://doi.org/10.1016/j.matpr.2021.10.106.

[45] I. Rezić, Prediction of the surface tension of surfactant mixtures for detergent formulation using Design Expert software, Monatsh Chem 142 (2011) 1219–1225. https://doi.org/10.1007/s00706-011-0554-y.

تطبيق منهجية سطح الاستجابة للتنبؤ بقوة الضغط للمونة الأسمنتية التي تحتوي على البوزولان الطبيعي

هاني أحمد داهش
قسم الهندسة المدنية، كلية الهندسة، جامعة القصيم، بريدة، المملكة العربية السعودية

أحمد فؤاد الراجي
قسم الهندسة المدنية، كلية الهندسة، جامعة القصيم، بريدة، المملكة العربية السعودية

تتناول هذه الورقة البحثية تأثير إضافة البوزولان الطبيعي (NP) كبديل جزئي للأسمنت و/أو الركام الناعم في مكعبات المونة الأسمنتية على مقاومة الضغط. وقد طُوّرت نماذج تنبؤية لمقاومة الضغط لمكعبات المونة الأسمنتية المحتوية على البوزولان الطبيعي باستخدام منهجية سطح الاستجابة(RSM) ، بالإضافة إلى إجراء تحسين متعدد الأهداف لزيادة مقاومة الضغط إلى أقصى حد ممكن عند استبدال الأسمنت بالبوزولان الطبيعي (NPC) بنسب تتراوح بين 0 و40% من وزن الأسمنت، واستبدال الرمل بالبوزولان الطبيعي (NPS) بنسب تتراوح بين 0 و40% من حجم الرمل. وللحد من التأثير السلبي للبوزولان الطبيعي على مقاومة الضغط، استُخدم غبار السيليكا (SF) كبديل جزئي للأسمنت بنسب وزنية تبلغ 5% و10%. تتضمن البيانات التجريبية مقاومة الضغط بعد 28 يومًا لعدد 23 خلطة مونة أسمنتية. عينات المونة الأسمنتية عبارة عن مكعبات بأبعاد 50×50×50 مم، وقد استُخدمت النتائج المعملية كقاعدة بيانات لتطوير نماذج تنبؤية لتقييم تأثير جرعة البوزولان الطبيعي وغبار السيليكا على مقاومة الضغط لمكعبات المونة الأسمنتية. خضعت النماذج المطورة للتقييم والتحقق من صحتها للتأكد من دلالتها وملاءمتها. تم تحليل تأثير كل مُعامل باستخدام تحليل التباين (ANOVA) ومقاييس إحصائية أخرى. تم تحديد العلاقات المثلى بين مقاومة الضغط ونسب البوزولان الطبيعي بديل الأسمنت (NPC) و/أو البوزولان الطبيعي بديل الرمل .(NPS) تم تحديد مستويات الاستبدال المثالية للبوزولان الطبيعي لتعزيز مقاومة الضغط لمكعبات المونة الأسمنتية من خلال التحسين العددي. توافقت نتائج النماذج المُنشأة بشكل جيد مع البيانات التجريبية. يتفوق النموذج التربيعي للتنبؤ بمقاومة الضغط لمكعبات المونة الأسمنتية على النموذج الخطي. يمكن للنماذج التي تم إنشاؤها في هذه الدراسة توقع مقاومة الضغط لمكعبات المونة الأسمنتية باستخدام البوزولان الطبيعي وغبار السيليكا.

Keywords in Arabic: مقاومة الضغط؛ البوزولان الطبيعي؛ غبار السيليكا؛ التنبؤ؛ منهجية سطح الاستجابة؛ التحسين